nature nanotechnology

ARTICLES

https://doi.org/10.1038/s41565-018-0271-3

A malaria vaccine adjuvant based on recombinant antigen binding to liposomes

Wei-Chiao Huang[1], Bingbing Deng[2], Cuiyan Lin[1], Kevin A. Carter[1], Jumin Geng[1], Aida Razi[3], Xuedan He[1], Upendra Chitgupi[1], Jasmin Federizon[1], Boyang Sun[1], Carole A. Long[2], Joaquin Ortega[3], Sheetij Dutta[4], C. Richter King[5], Kazutoyo Miura[2], Shwu-Maan Lee[5] and Jonathan F. Lovell[1]*

Pfs25 is a malaria transmission-blocking vaccine antigen candidate, but its apparently limited immunogenicity in humans has hindered clinical development. Here, we show that recombinant, polyhistidine-tagged (his-tagged) Pfs25 can be mixed at the time of immunization with pre-formed liposomes containing cobalt porphyrin–phospholipid, resulting in spontaneous nanoliposome antigen particleization (SNAP). Antigens are stably presented in uniformly orientated display via his-tag insertion in the cobalt porphyrin–phospholipid bilayer, without covalent modification or disruption of antigen conformation. SNAP immunization of mice and rabbits is well tolerated with minimal local reactogenicity, and results in orders-of-magnitude higher functional antibody generation compared with other 'mix-and-inject' adjuvants. Serum-stable antigen binding during transit to draining lymph nodes leads to enhanced antigen uptake by phagocytic antigen-presenting cells, with subsequent generation of long-lived, antigen-specific plasma cells. Seamless multiplexing with four additional his-tagged *Plasmodium falciparum* polypeptides induces strong and balanced antibody production, illustrating the simplicity of developing multistage particulate vaccines with SNAP immunization.

An effective malaria vaccine would be instrumental in eliminating the disease, which causes over 200 million cases and nearly half a million deaths annually[1]. One unique approach is a transmission-blocking vaccine (TBV). TBVs cause immunized hosts to transfer induced antibodies to mosquitos during a blood meal, blocking parasite development in the mosquito gut. A vaccine that reduces parasite transmission is part of the World Health Organization Malaria Vaccine Technology Roadmap, but has not yet been evaluated in large-scale trials, due in part to challenges in developing a TBV that produces high and sustained levels of transmission-blocking antibodies[2,3].

Plasmodium falciparum Pfs25 is an intensively studied TBV antigen candidate[4–6]. The 25 kDa protein contains 11 disulfide bonds, so the production of properly folded Pfs25 is of interest[7–10]. Clinical trials with Pfs25 or *Plasmodium vivax* Pvs25 have failed to produce satisfactory levels of antibodies using alum as a vaccine adjuvant, and the use of Montanide ISA 51 as an adjuvant resulted in unexpected local reactogenicity[11,12]. The limited immunogenicity of Pfs25 may be related to its compact structure and putative hapten-like behaviour[13].

Antigen engineering has been pursued to improve the induction of antibodies against Pfs25. This includes: conjugation to protein toxins (from *Pseudomonas*[14], cholera[15,16] or tetanus[13]); conjugation to nanoparticles (such as gold[17] or polymer[18]); engineering Pfs25 in virus-like particles[19]; and the use of viral vectors[20]. Emerging approaches include the use of recombinant protein tags for downstream Pfs25 multimerization[21] or attachment to virus-like particles[22]. While these strategies hold potential, genetically engineered constructs or conjugation strategies are time- and resource-consuming, can induce heterogeneous antigen populations, can mask important epitopes, risk incorrect folding and can impede target antigen characterization within the resulting constructs.

Liposomes containing cobalt porphyrin–phospholipid (CoPoP) can be stably functionalized by simple mixing with proteins bearing a polyhistidine-tag (his-tag)—a small 6–10 stretch of histidine residues used in recombinant protein purification[23]. A carboxy (C)-terminal his-tagged and glycosylation-free Pfs25 was recently produced in a baculovirus system[10]. The 11 disulfide bonds of this protein match the predicted structure of the analogous *P. vivax* Pvs25[24]. Here, we make use of this well-characterized his-tagged antigen for spontaneous nanoliposome antigen particleization (SNAP). Spontaneous particleization (that is, binding of soluble, recombinant antigens to nanoliposomes so that they decorate the surface of the colloidal particles) occurs when the antigens stably bind to membranes via insertion and coordination of the his-tag into bilayers containing CoPoP.

SNAP

We formed liposomes with two active lipids—a synthetic monophosphoryl lipid A (phosphorylated hexaacyl disaccharide (PHAD); a toll-like receptor 4 agonist) and CoPoP, which is biologically inert but confers spontaneous his-tag antigen particelization. Two passive lipids completed the formulation—1,2-dipalmitoyl-*sn*-glycero-3-phosphocholine (DPPC) and cholesterol. Liposomes were produced with a mass ratio of 4:2:1:1 of DPPC:cholesterol:CoPoP:PHAD unless otherwise indicated. Native polyacrylamide gel electrophoresis showed that, with simple mixing, Pfs25 bound to liposomes containing CoPoP, but not to liposomes containing porphyrin–phospholipid (PoP), which are identical but lack cobalt (Fig. 1a). Liposomes containing a nickel-chelated

[1]Department of Biomedical Engineering, University at Buffalo, State University of New York, Buffalo, NY, USA. [2]Laboratory of Malaria and Vector Research, National Institute of Allergy and Infectious Diseases, National Institutes of Health, Rockville, MD, USA. [3]Department of Anatomy and Cell Biology, McGill University Montreal, Quebec, Canada. [4]Walter Reed Army Institute of Research, Silver Spring, MD, USA. [5]PATH's Malaria Vaccine Initiative, Washington, DC, USA. *e-mail: jflovell@buffalo.edu

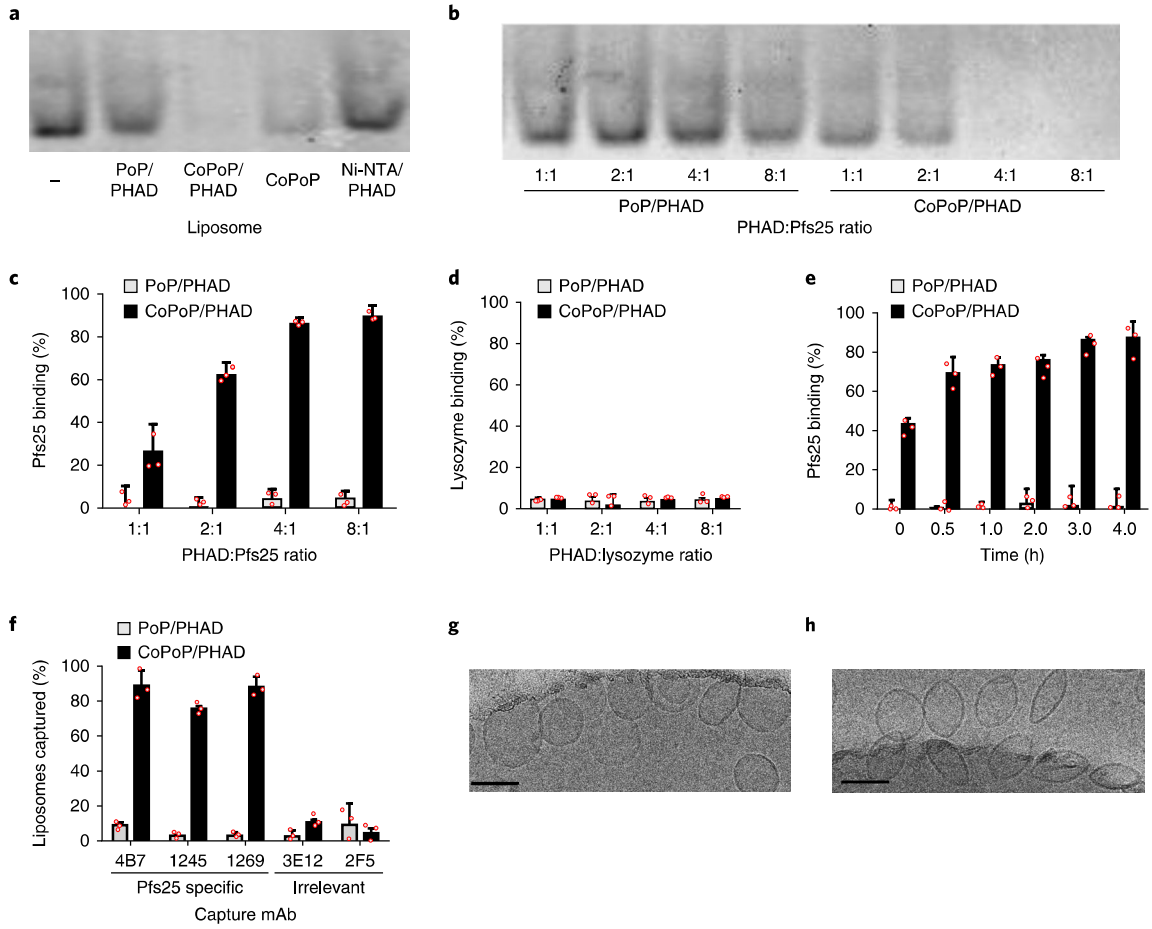

Fig. 1 | SNAP with his-tagged Pfs25. a, Native PAGE of his-tagged Pfs25 after 3 h incubation with the indicated liposomes at a 4:1 PHAD:protein (or analogous) ratio. **b**, Native PAGE of 1 μg Pfs25 incubated with varying liposome amounts. **c**,**d**, Protein binding determined by microcentrifugal filtration using Pfs25 (**c**) or non-his-tagged lysozyme (**d**). **e**, Kinetics of Pfs25 binding to PoP or CoPoP liposomes at room temperature. **f**, Immunoprecipitation of Pfs25-bound liposomes by Pfs25-specific mAbs. **g**,**h**, Cryo-electron micrographs of CoPoP/PHAD liposomes with (**g**) or without (**h**) incubation with Pfs25 for 3 h. Scale bars: 100 nm. The data in **a** and **b** are representative of $n = 3$ independent experiments. Bar graphs in **c**–**f** show means ± s.d. for $n = 3$ independent experiments.

headgroup lipid (Ni-NTA) did not stably bind Pfs25. With CoPoP, the his-tag buries itself within the hydrophobic cobalt porphyrin bilayer and coordinates with the metal, resulting in attachment that is stable in biological media. Liposomal Ni-NTA approaches for binding his-tagged ligands are unstable in biological media[23,25,26]. Liposomal Co-NTA has been explored for immunization, but the approach was found to be inferior to covalent linkage[27]. We previously found that Co-NTA cannot stably bind his-tagged peptides[23].

When varying amounts of CoPoP/PHAD liposomes were incubated with Pfs25, a 4:1 mass ratio of PHAD to protein was sufficient for binding (Fig. 1b). This is equivalent to a CoPoP:Pfs25 mass ratio of 4:1 and a lipid:Pfs25 mass ratio of 32:1. Pfs25 did not bind PoP/PHAD liposomes. A similar trend was observed with a microcentrifugal filtration binding assay (Fig. 1c,d). Lysozyme—a protein without a his-tag—did not bind to CoPoP liposomes (Fig. 1d). Approximately 80% Pfs25 binding was achieved at room temperature in 3 h (Fig. 1e). These particleization conditions (4:1 mass ratio of CoPoP (320 μg ml^{-1}) to Pfs25 (80 μg ml^{-1}), combined in equal volume and incubated without shaking at room temperature for 3 h) were fixed for all studies, and the desired dosing was achieved by subsequent dilution in buffered saline.

His-tagged Pfs25 exhibited a low α-helical content based on circular dichroisim, consistent with the structure of the same protein in an antibody complex (Supplementary Fig. 1)[28]. Following Pfs25 binding to CoPoP liposomes, we assessed whether monoclonal antibodies (mAbs) recognized the correctly folded protein conformation. 4B7 has been reported to be a conformational-specific mAb[4]. Recently, two non-overlapping epitopes have been identified by functional mAbs (1269 and 1245)[28]. The 1269 mAb binds to a similar epitope as 4B7, while 1245 binds a distinct region. Following incubation with Pfs25-specific mAbs, protein G beads were used to immunoprecipitate the entire liposome–antigen complex, which was then detected by endogenous PoP or CoPoP fluorescence following detergent disruption. As shown in Fig. 1f, 4B7, 1269 and 1245 immunoprecipitated whole CoPoP liposomes bound with his-tagged Pfs25, but not PoP liposomes (which do not bind Pfs25). As both 1269 and 1245 bind to Pfs25 in a reduction-sensitive fashion, these results suggest that particleized Pfs25 maintains a correct conformation. A mAb against a human immunodeficiency virus envelope segment (2F5) and another TBV antigen, Pfs48/45 (3E12), served as negative controls.

Cryo-electron microscopy revealed that CoPoP/PHAD liposomes were small and unilamellar, with a spherical size close to 100 nm (Fig. 1g). Following Pfs25 binding, liposome curvature changed subtly, forming more oblong structures (Fig. 1h). Individual proteins were not visible due to their small size. Based on light scattering, the liposomes were approximately 100 nm in diameter (Supplementary Fig. 2a). Minimal change in size or

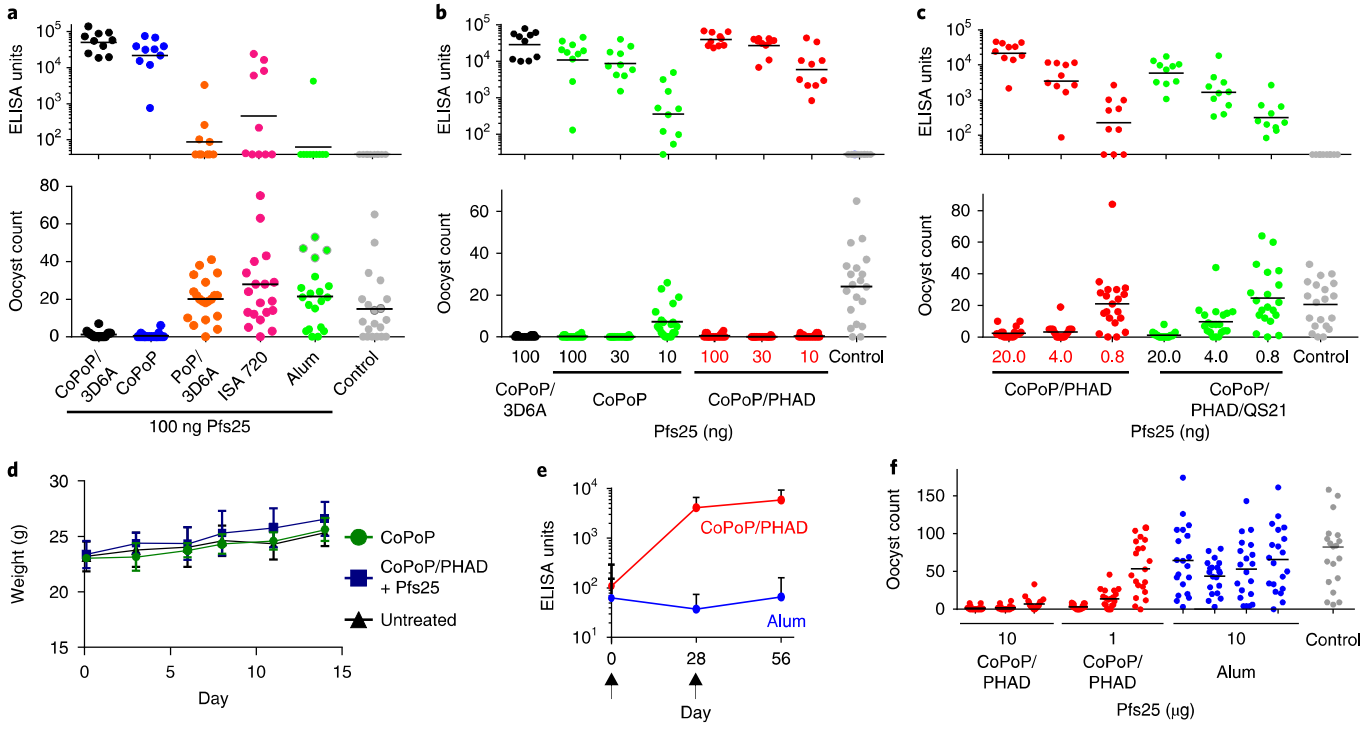

Fig. 2 | Pfs25 SNAP immunization in mice and rabbits. a–c, Anti-Pfs25 IgG ELISA data (top) and SMFA results (bottom). Mice were intramuscularly immunized on days 0 and 21 with the indicated Pfs25 doses, and serum was collected on day 42 and assessed. **a**, Immunization with 100 ng Pfs25, mixed with the indicated adjuvants just before injection. **b**, Dose de-escalation of Pfs25 with CoPoP or CoPoP/PHAD liposomes. **c**, Dose de-escalation of Pfs25 with CoPoP/PHAD liposomes with or without QS21. Control groups correspond to various CoPoP adjuvants without Pfs25. **d**, Mouse weight following extreme CoPoP dosing. CoPoP-only liposomes were intravenously injected at a CoPoP dose of 100 mg kg^{-1} (>100,000-fold excess over the functional CoPoP dose). Another group of mice was given a single vaccination of 20 μg Pfs25 adjuvanted with CoPoP/PHAD (5,000-fold excess over the functional vaccine dose) at the standard 1:4 Pfs25:PHAD ratio. Means ± s.d. are shown for $n = 5$ mice. **e**, IgG ELISA titre in rabbits immunized with 10 μg Pfs25 at the time points indicated by arrows. Geometric means ± s.d. are shown for $n = 3$ (CoPoP/PHAD) or $n = 4$ (alum) rabbits. **f**, SMFA results, following immunization, of the serum of individual rabbits as indicated. The ELISA experiments in **a–c** were performed with $n = 10$ independent mice, and lines show the geometric mean. The SMFA experiments in **a–c** and **f** were performed with $n = 20$ mosquitos, and lines show the arithmetic mean. A fixed PHAD:Pfs25 mass ratio of 4:1 (or equivalent) was maintained in all experiments.

polydispersity was induced by SNAP (Supplementary Fig. 2a,b). SNAP did not substantially impact the CoPoP/PHAD liposome surface charge (Supplementary Fig. 2c), which had a negative zeta potential, consistent with other observations of liposomes containing monophosphoryl lipid A[29].

Refrigerated storage stability was assessed over nine months. Minimal change was observed in liposome size, which was close to 100 nm (Supplementary Fig. 3a), or polydispersity index, which remained less than 0.1 (Supplementary Fig. 3b). The spontaneous Pfs25 binding capacity of the liposomes remained intact throughout (Supplementary Fig. 3c). Four separate batches of CoPoP/PHAD liposomes exhibited similar size, polydispersity and capacity for Pfs25 binding (Supplementary Fig. 3d–f).

Antigen particleization induces strong antibody responses

Mice were immunized intramuscularly with 100 ng of Pfs25, mixed just before vaccination with alum, Montanide ISA 720, CoPoP liposomes or CoPoP/(3-deacyl)-(6-acyl) PHAD (3D6A) liposomes. 3D6A is a structurally similar form of PHAD used in our initial immunization studies. In all immunizations, a fixed mass ratio for PHAD:Pfs25 of 4:1 was used. No additional purification steps were taken after combining the antigen with the adjuvants. As shown in Fig. 2a, all CoPoP liposomes induced the production of immunoglobulin G (IgG) that was functional in a standard membrane-feeding assay (SMFA). Liposomes lacking cobalt produced orders-of-magnitude lower anti-Pfs25 IgG and did not induce SMFA activity (Supplementary Table 1). At 100 and 30 ng dosing, both CoPoP/PHAD liposomes and CoPoP liposomes induced strong IgG and full SMFA activity (Fig. 2b and Supplementary Table 2). However, at a 10 ng dose of Pfs25, only CoPoP/PHAD liposomes induced antibody production with full SMFA activity. At 100 ng Pfs25, inclusion of PHAD resulted in higher production of IgG2a and a higher IgG2a:IgG1 ratio compared with CoPoP liposomes lacking PHAD (Supplementary Fig. 4a,b).

Further dose de-escalation was performed in mice. CoPoP/PHAD liposomes that included the saponin QS21 were also examined. With this DPPC-based formulation, QS21 induced liposome aggregation, although Pfs25 binding was not impaired (Supplementary Fig. 5). Addition of QS21 did not enhance Pfs25 antibody production (Fig. 2c) and appeared to decrease IgG2a production (Supplementary Fig. 4c,d). CoPoP/PHAD liposomes induced antibodies that were effective in the SMFA at antigen doses down to 4 ng (Supplementary Table 3). This corresponds to 16 ng of PHAD, which is 1,000-fold lower than what is typically used for murine immunization[29].

Safety studies were carried out using high doses of CoPoP. To ascertain whether CoPoP itself is tolerated, we formed CoPoP liposomes with 95 mol% CoPoP, along with 5% polyethylene glycol distearoylphosphoethanolamine (PEG-lipid) for colloidal stability. CoPoP liposomes were then directly injected intravenously

into mice at a dose of 100 mg kg^{-1} (CoPoP). This CoPoP dose was approximately 138,000 times higher than the minimum dose administered to mice that induced functional SMFA activity (4 ng Pfs25 and 16 ng CoPoP). Another group of mice was injected intramuscularly with a single dose of 20 µg Pfs25 adjuvanted with CoPoP/PHAD liposomes, corresponding to a 5,000-fold higher dose than the minimum functional dose. Mice exhibited normal weight gain (Fig. 2d). A complete blood cell count (Supplementary Fig. 6a) and serum chemistry panel analysis (Supplementary Fig. 6b) two weeks following treatment revealed no statistically significant differences compared with healthy mice. No obvious differences in the liver, lungs, kidney or spleen of mice were observed with histology (Supplementary Fig. 6c). Thus, CoPoP liposomes appear to be well tolerated, although additional toxicity studies are required. Vitamin B12—a cobalt(III) porphyrin-related macrocycle—has been administered intravenously to healthy human volunteers at 5 g dosing[30], as well as with repetitive milligram intramuscular dosing[31].

To assess whether SNAP immunization elicits transmission-blocking antibodies in rabbits, intramuscular immunization was carried out with 10 µg of Pfs25 on days 0 and 28. When mixed with CoPoP/PHAD liposomes, but not alum, strong anti-Pfs25 IgG titres were induced by day 56, and also pre-boost on day 28 (Fig. 2e). The post-immune sera from the rabbits immunized with SNAP, but not alum, produced transmission-blocking activity in the SMFA (Fig. 2f and Supplementary Table 5). Even at a tenfold lower antigen dose of 1 µg Pfs25 (4 µg PHAD), transmission-blocking antibody activity was induced in two of three rabbits immunized with SNAP.

Vaccine mechanism

Next, we sought to elucidate mechanistic insights into SNAP immunization, which is hypothesized to operate at multiple steps of immune activation (Fig. 3a). Serum-stable antigen particleization enables intact transit of the antigen–liposome complexes to draining lymph nodes, where they are more avidly taken up by immune cells. Additional factors, including recruitment of immune cells to the draining lymph nodes and downstream activation of dendritic cells, probably contribute to the formation of germinal centres, the recruitment of T-follicular helper (Tfh) cells and, ultimately, the generation of long-lived, antigen-specific plasma cells.

To monitor antigen–adjuvant association, Pfs25 was labelled with the fluorescent dye Oyster 488, generating Pfs25-488. When Pfs25-488 was incubated with CoPoP/PHAD liposomes, but not PoP/PHAD liposomes, fluorophore proximity to the CoPoP chromophore induced fluorescence quenching. When incubated in human serum for 2 wk at 37 °C, Pf25-488 binding to CoPoP/PHAD liposomes remained intact, whereas no binding occurred with PoP/PHAD liposomes (Fig. 3b). Following the 2 wk incubation period, fluorescence of the dye could be restored upon dissociation (Supplementary Fig. 7a,b). Binding was also stable in bovine serum (Supplementary Fig. 7c).

To investigate the innate response, 100 ng Pfs25 was mixed with CoPoP/PHAD liposomes or alum and intramuscularly administered to mice. Immune cell recruitment in draining lymph nodes was measured 48 h following injection using a flow cytometry discrimination approach (Supplementary Fig. 8a)[32,33]. CoPoP/PHAD liposomes induced higher recruitment of macrophage and infiltrating monocytes compared with alum (Fig. 3c). Increased levels of CD11b$^-$ dendritic cells were noted in both the alum and CoPoP/PHAD liposome groups. Cd11b$^-$ dendritic cells play a role in cellular adaptive immune responses[34–36]. In immunized mice, splenocytes produced interferon gamma when incubated with the antigen, demonstrating the involvement of T cells (Supplementary Fig. 9). Other immune cell types (eosinophils, neutrophils, CD11b^{low} dendritic cells and myeloid dendritic cells) did not increase in draining lymph nodes. The increased levels of certain immune cells in the draining lymph nodes, by just two- to threefold, do not fully account for the drastic enhancement in antibody production induced by SNAP.

Following injection of fluorescently labelled Pfs25-488, lymphatic antigen drainage was modulated relative to alum, resulting in greater lymph node accumulation, which may have some positive impact on immunogenicity (Supplementary Fig. 10). However, the enhanced lymph node biodistribution of only several fold does not account for the greater antibody response by several orders of magnitude.

Next, the uptake of the antigen–liposome complex into antigen-presenting cells (APCs) was examined in vitro using fluorescence microscopy (Fig. 3d). When Pfs25-488 was incubated with RAW264.7 murine macrophages, no cellular antigen uptake was observed. No antigen uptake was observed when Pfs25-488 was mixed with PoP/PHAD liposomes. However, the fluorescence of the liposomes themselves was detected, since macrophages avidly uptake liposomes[37,38]. When Pfs25 was presented on liposomes using SNAP with CoPoP/PHAD liposomes, both antigen and liposome uptake occurred. Quantitative measurement of Pfs25 uptake confirmed this trend in both murine macrophages and murine bone-marrow-derived dendritic cells (BMDCs)—another class of APCs (Fig. 3e). In the presence of cytochalasin B (a phagocytosis inhibitor), diminished Pfs25 uptake occurred, suggesting a phagocytic uptake mechanism.

Next, we examined whether enhanced uptake of Pfs25 in APCs occurred in draining lymph nodes. As shown in Fig. 3f and Supplementary Fig. 11, 2 d following SNAP immunization of mice, Pfs25 was taken up in all major types of APCs, including B cells (B220), macrophages (F4/80), dendritic cells (CD11c) and major histocompatibility complex II (MHC-II)-expressing cells (I-A/I-E). In contrast, when adjuvanted with alum, ISA 720 or non-particleizing PoP/PHAD liposomes, there was minimal Pfs25 uptake into most APC types. Thus, improved delivery to APCs appears to be a key mechanism in which SNAP exerts enhanced immunogenicity compared with other adjuvants.

Maturation of dendritic cells involves upregulation of surface receptors, including CD40 and CD80. When BMDCs were incubated with Pfs25 for 24 h, CD40 and CD80 production increased when the antigen was combined with CoPoP/PHAD liposomes, compared with the protein alone or liposomes lacking PHAD (Fig. 3g and Supplementary Fig. 12). PHAD has been shown to stimulate BMDC activation[39]. Thus, concomitant dendritic cell activation by PHAD may provide an additional mechanism of enhanced immune response.

Germinal centre cell formation and the recruitment of Tfh cells were assessed. Germinal centre B cells were identified by gating on B220$^+$ cells and examining CD95$^+$GL7$^+$ cells (Supplementary Fig. 13). Tfh cells were gated on CD4$^+$, then identified with PD1$^+$CXCR5$^+$ staining (Supplementary Fig. 14). One week following murine intramuscular immunization, when combined with CoPoP/PHAD liposomes, Pfs25 induced a higher number of germinal centre B cells and Tfh cells in draining lymph nodes (Fig. 3h,i). There was no increase in these cell populations when Pfs25 was administered with alum.

Efficacy of SNAP immunizationAdditional adjuvants

The durability of the antibody response for a TBV is important. A recent study using Pfs25–toxin conjugates reported antibody half-lives in the 50–100 d range[13]. Following SNAP immunization with 100 ng Pfs25, antibody levels did not decrease to half of the day 42 levels by day 250, corresponding to an antibody half-life of greater than 250 d (Fig. 4a). Antigen-specific, long-lived plasma cells (CD138$^+$B220$^-$) were detected in the bone marrow of mice on day 250 (Fig. 4b and Supplementary Fig. 15), confirming an immunological basis for the long-lived antibody response. Serum drawn from mice at day 250 was active in transmission blocking based on the SMFA (Fig. 4c).

Additional adjuvants were compared with CoPoP/PHAD in a head-to-head study. Commercial adjuvants included alum, TiterMax, Adju-Phos, Quil-A, Sigma Adjuvant System, AddaVax (similar to MF59) and Freund's Adjuvant (Complete Freund's

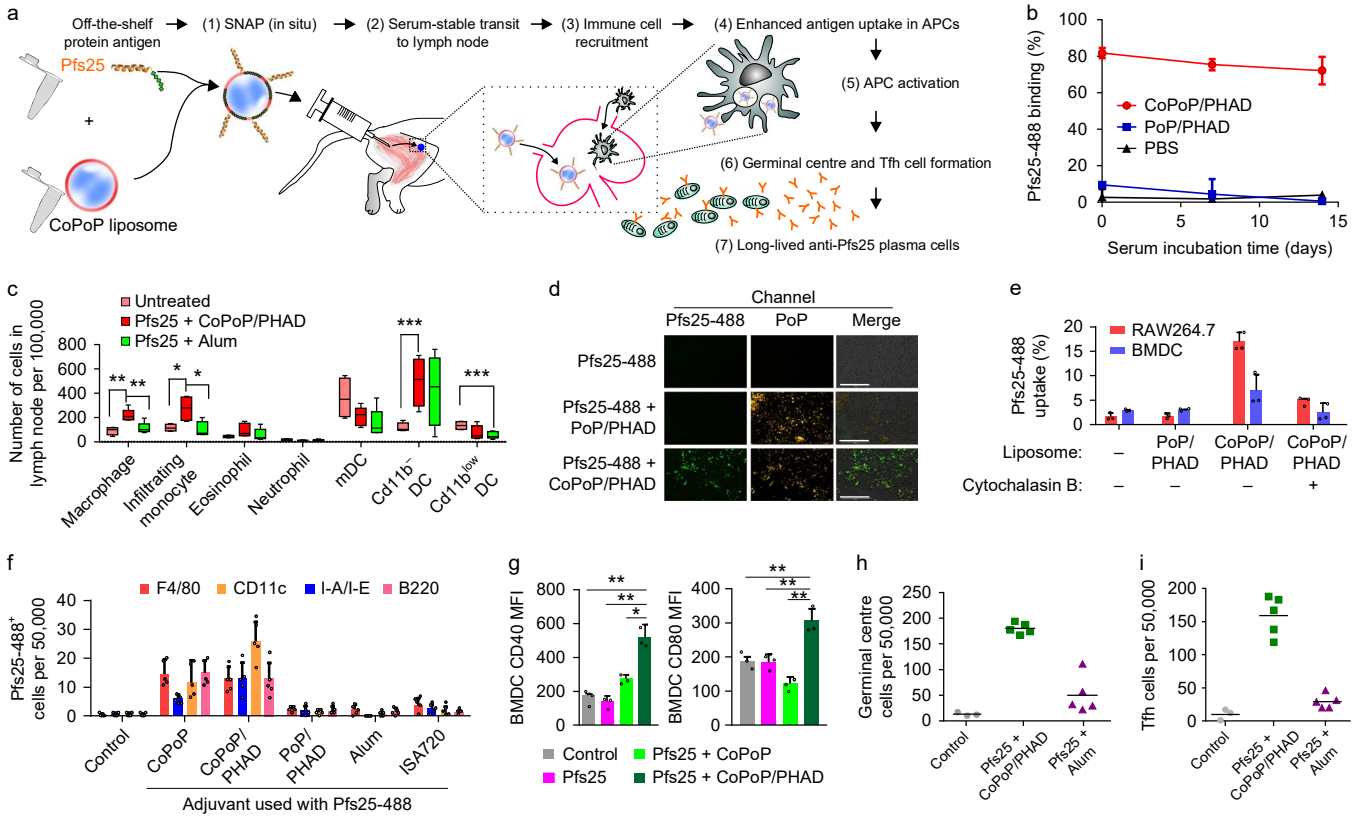

Fig. 3 | Mechanistic insights into SNAP immunization. a, Putative steps in SNAP immunization. **b**, Particleization stability in 20% human serum at 37 °C. Lines show means ± s.d. for $n = 3$ experiments. **c**, Immune cell populations in draining lymph nodes 48 h after intramuscular Pfs25 immunization. Data show box-and-whiskers plots ($n = 5$ mice per group). The line represents the median, the whiskers show the data range and the box shows the interquartile range. DC, dendritic cell; mDC, myeloid DC. **d**, Fluorescence microscopy of RAW264.7 macrophages after incubation with Pfs25 and liposomes. Scale bars: 100 µm. Representative images from $n = 3$ independent experiments are shown. **e**, Pfs25 uptake following incubation with murine RAW264.7 cells or BMDCs. Cytochalasin B was used as a phagocytosis inhibitor. **f**, Pfs25 uptake in immune cells in the draining lymph nodes of mice 48 h after intramuscular administration. Lymph node cells were assessed for Pfs25-488 uptake with flow cytometry and co-staining with the indicated surface markers. Bars show means ± s.d. for $n = 5$ mice per group. **g**, Activation of BMDCs as assessed by CD40 (left) or CD80 (right) mean fluorescence intensity (MFI) following incubation with 1 µg ml^{-1} of Pfs25 for 24 h. **h**,**i**, Germinal centre cells (GL7$^+$CD95$^+$; within the B220$^+$ cell population) (**h**) and Tfh cells (CXCR5$^+$PD-1$^+$; within the CD4$^+$ cell population) (**i**) in draining lymph nodes 7 d after intramuscular immunization with 100 ng Pfs25. In **e** and **g**, values show means ± s.d. for $n = 3$ biologically independent experiments. In **h** and **i**, lines show means for $n = 5$ mice per group. Asterisks show significance as determined by unpaired, two-tailed Student's *t*-test: $^*P < 0.05$; $^{**}P < 0.01$; $^{***}P < 0.005$.

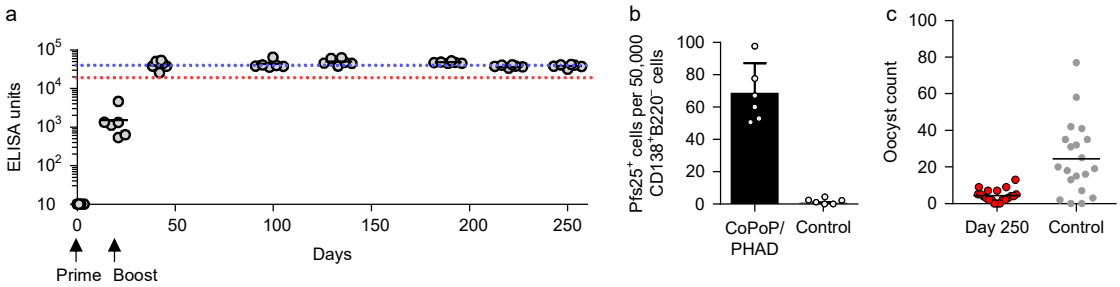

Fig. 4 | Durability of the anti-Pfs25 IgG response with SNAP immunization. Mice were immunized intramuscularly with 100 ng Pfs25 mixed with CoPoP/PHAD liposomes (400 ng PHAD) on days 0 and 21, as indicated by the arrows in **a**. **a**, Serum was sampled periodically and assessed for anti-Pfs25 IgG. The blue and red lines show the 4×10^4 and 2×10^4 points on the *y* axis, respectively. Black lines show geometric means for $n = 6$ mice. **b**, On day 250, bone marrow was assessed for antigen-specific, long-lived plasma cells by flow cytometry (CD138$^+$B220$^-$; staining positive for intracellular binding to fluorescent Pfs25). Bars show means ± s.d. for $n = 6$ mice per group. **c**, Pooled mouse serum collected from mice on day 250 and assessed with SMFA. Lines show means for $n = 20$ mosquitos per group.

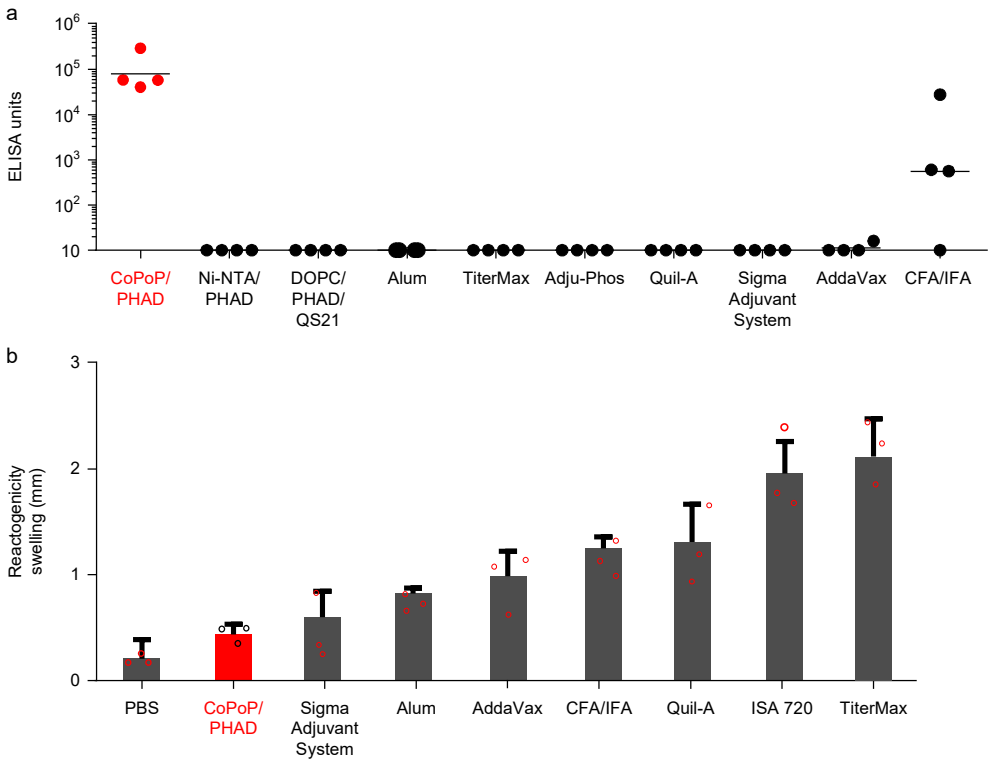

Fig. 5 | Immunization potency and local reactogenicity of SNAP compared with other adjuvants (all mixed before injection). **a**, Comparison of anti-Pfs25 IgG titres for 100 ng Pfs25 vaccinated with the indicated adjuvants, which were combined with Pfs25 before injection. Each ELISA point represents the anti-Pfs25 IgG titre of an individual mouse. Lines show geometric means for $n = 4$ mice per group. CD-1 mice were vaccinated intramuscularly, with priming on day 0, boosting on day 21 and serum collection on day 42. DOPC, 1,2-dioleoyl-sn-glycero-3-phosphocholine. **b**, Local reactogenicity of 100 ng Pfs25 injected in the footpad of CD-1 mice as measured by swelling. Bar graph shows mean ± s.d. for $n = 3$ mice per group.

Adjuvant (CFA)/Incomplete Freund's Adjuvant (IFA)). A 100 nm formulation containing dioleoylphosphatidylcholine, PHAD and QS21 was prepared with a similar composition to AS01 (ref. [40]). Only the CoPoP/PHAD adjuvant induced high levels of Pfs25 antibodies with 100 ng Pfs25, presumably owing to the importance of antigen particleization (Fig. 5a). Despite the potent response, CoPoP/PHAD liposomes with Pfs25 produced the least amount of local reactogenicity of all the adjuvants assessed when injected intradermally in the footpad, as assessed by swelling (Fig. 5b).

The effect of Pfs25 density on the liposomes was assessed with a low dose (10 ng) of Pfs25. Density was compared under standard conditions (estimated at 121 proteins per liposome based on protein binding, liposome diameter and geometrical considerations[41]) and a reduced density of just 5% of that amount (6 proteins per liposome). The higher-density antigen resulted in more production of anti-Pfs25 IgG by approximately one order of magnitude (Supplementary Fig. 16a). However, post-immune sera for both high and low antigen density fully inhibited parasite development in the SMFA (Supplementary Fig. 16b), implying that a sufficient level of antibodies was induced to saturate the assay. We conclude that the SNAP approach is effective at generating functional antibodies over a wide range of antigen densities, even at low antigen injected doses.

The use of CoPoP/PHAD liposomes that are combined with separately produced antigen at the time of immunization may have advantages in modular research and early-phase clinical trials, since only a single batch of sterile liposomes would be required. However, it could eventually be beneficial to develop a single vial formulation without the requirement of a mixing step. We assessed whether Pfs25, once bound to CoPoP/PHAD liposomes, would be a stable formulation. As shown in Supplementary Fig. 17a–c, Pfs25 binding remained intact over one month, as did liposome size and polydispersity. No free protein was detected by native polyacrylamide gel electrophoresis (PAGE) following six weeks of storage (Supplementary Fig. 17d). When electrophoresis was performed under reducing and denaturing conditions (which triggers release of the his-tagged protein), no Pfs25 degradation was observed (Supplementary Fig. 17e). Pfs25 that was pre-incubated for multiple weeks at 4 °C before vaccination (100 ng for both the prime and boost) induced no difference in IgG generation (Supplementary Fig. 17f). Thus, the SNAP approach could be applicable to both bedside mixing and generation of batches of particleized antigens.

Antigen multiplexing

The multistage life cycle of *Plasmodium* species, in which different proteins are exposed on the parasite surface at different stages, may be a contributing factor to the difficulty of creating an effective malaria vaccine. Multistage, multi-antigen malaria vaccines are considered to be a promising avenue of research[42]. However, the process of developing and biochemically characterizing multistage, multi-antigen vaccines is challenging. CoPoP/PHAD liposomes could facilitate this process since well-defined his-tagged antigens can easily be mixed with the liposomes to undergo SNAP. The antigen composition would be easily adjustable and no chemical conjugation or purification steps are required.

We examined a panel of his-tagged *P. falciparum* antigens expressed at different stages of the parasite life cycle. The concept is that these antigens could all be combined into a single particle by simple mixing before immunization (Fig. 6a). Apical membrane antigen-1 (AMA-1) is a blood-stage antigen candidate expressed inside schizonts[43]. Pfg27 is produced in gametocytes[44]. Pfs230 is an

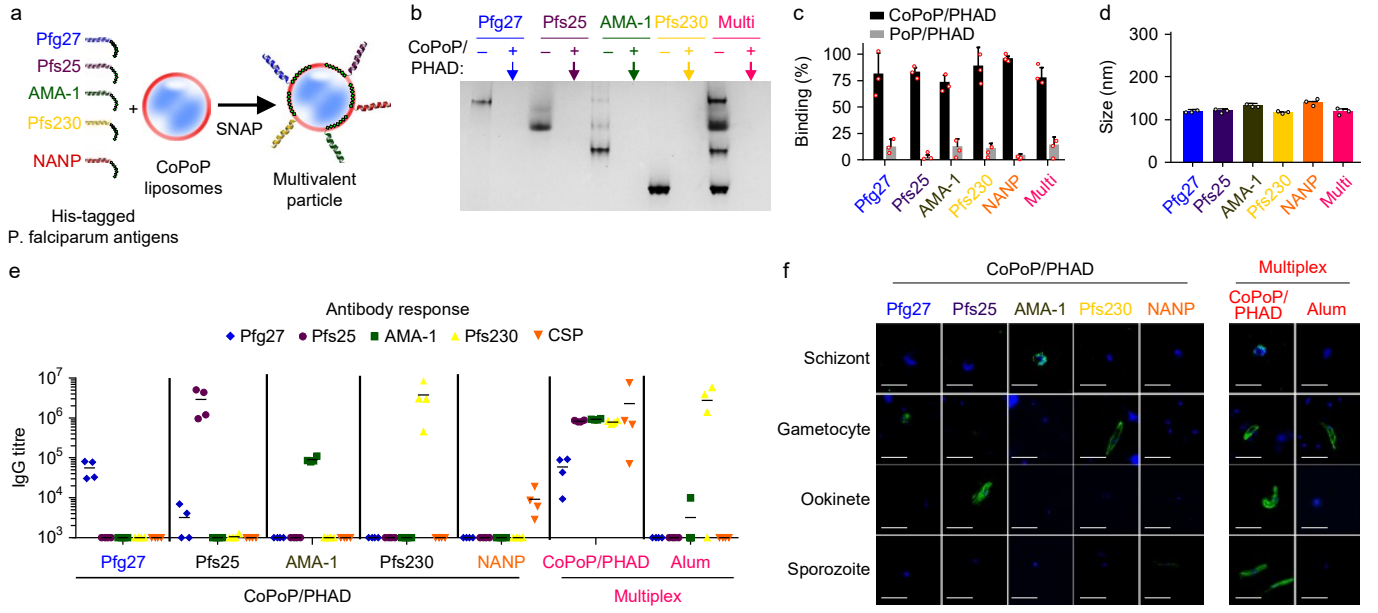

Fig. 6 | Multiplexed SNAP with P. falciparum antigens. a, Schematic representation of multivalent SNAP. **b**, Native PAGE demonstrates effective single and multiplexed antigen binding to CoPoP/PHAD liposomes. The absence of a protein band indicated by the arrow reflects antigen binding to the liposomes, which are too large to enter the gel. **c**, Single and multiplexed antigen binding as assessed by microcentrifugal filtration. **d**, Size of liposomes following SNAP. **e**, ELISA against the indicated antigens in mice immunized with individual antigens or a multiplexed combination of all antigens. Lines show geometric means for $n = 4$ mice per group. **f**, Immunofluorescence assays of the indicated post-immune sera with fixed parasites. Scale bars: 10 µm. For **c** and **d**, error bars show means ± s.d. for $n = 3$ independent experiments. **b** and **f** show representative results of $n = 3$ independent experiments. 'Multi' represents the multiplexed combination.

antigen candidate expressed in sexual-stage gametocytes and gametes. The NANP peptide (Asn-Ala-Asn-Pro) is a repeating sequence derived from the circumsporozoite protein (CSP)—a pre-erythrocytic-stage antigen expressed on sporozoites.

The binding of each his-tagged protein antigen (Pfg27, Pfs25, Pfs230 and AMA-1), as well as the multiplexed combination, was assessed using native PAGE (Fig. 6b). When incubated with CoPoP/PHAD liposomes, the proteins bound efficaciously, and no free protein bands were seen on the gel. The proteins had appropriate sizes and charges to enable the multiplexed antigen binding to also be confirmed with individually resolved antigens. Microcentrifugal filtration confirmed the binding of each antigen to CoPoP/PHAD liposomes, but not identical liposomes lacking cobalt (Fig. 6c). Following antigen binding, the size of the multiplexed liposomes remained around 100 nm (Fig. 6d), and the polydispersity was less than 0.3 (Supplementary Fig. 18). Thus, CoPoP liposomes are amenable for SNAP of multiple antigens simultaneously.

Mice were immunized with 100 ng of each antigen, either individually or multiplexed. A fixed mass ratio of PHAD:antigens of 4:1 was used in all cases. When immunized with individual antigens, specific IgG was induced for all antigens without cross-reactivity (Fig. 6e). The multiplexed SNAP vaccine resulted in high IgG production against all the antigens. Alum was ineffective for multiplexing antigens, with significant IgG levels only detected for one (out of five) antigens: Pfs230. Analysis of the SNAP multiplexed response revealed a slight decrease in the IgG levels against Pfs25 and Pfs230 compared with their single antigen vaccination counterparts. In contrast, there was a substantial increase in the anti-CSP IgG titre of the multiplexed vaccine. A duplex vaccine of Pfs25 combined with NANP was sufficient to generate increased levels of anti-CSP IgG (Supplementary Fig. 19).

Next, we investigated whether multiplexed SNAP immunization induced antibodies that recognize native *P. falciparum* proteins. Different life stages of the parasite, including sporozoites, ookinetes, gametocytes and schizonts, were subjected to an immunofluorescence assay. Post-immune sera from mice immunized with individual his-tagged antigens exhibited expected patterns of reactivity for the individual life stages of parasites (Fig. 6f and Supplementary Fig. 20). The post-immune sera from mice SNAP immunized with multivalent antigens recognized all expected life stages of the parasite. Multiplexed antigens adjuvanted with alum did not induce effective antibodies, with the only response being observed with Pfs230. The mechanism by which SNAP immunization exerts a balanced immune response requires further characterization, but may relate to the low antigen dose used, or improved and balanced antigen uptake in APCs.

Conclusion

Recombinant his-tagged proteins spontaneously bind to liposomes containing CoPoP. This enables the rapid, gentle and uniformly oriented particleization of well-characterized, purified his-tagged antigens. The SNAP approach safely induced durable antibody responses orders of magnitude greater than other adjuvants. In mice, functional antibodies were induced with nanograms of Pfs25, showing potential for antigen-sparing practices. SNAP immunization was well suited for multiplexed immunization with at least five his-tagged antigens—an approach that may be of interest for developing recombinant vaccines that target different life stages of the malaria parasite.

Online content

Any methods, additional references, Nature Research reporting summaries, source data, statements of data availability and associated accession codes are available at https://doi.org/10.1038/s41565-018-0271-3.

Received: 22 January 2018; Accepted: 3 September 2018;
Published online: 08 October 2018

References

1. *WHO World Malaria Report 2017* (World Health Organization, 2017).
2. Nunes, J. K. et al. Development of a transmission-blocking malaria vaccine: progress, challenges, and the path forward. *Vaccine* **32**, 5531–5539 (2014).
3. Birkett, A. J. Status of vaccine research and development of vaccines for malaria. *Vaccine* **34**, 2915–2920 (2016).
4. Barr, P. J. et al. Recombinant Pfs25 protein of *Plasmodium falciparum* elicits malaria transmission-blocking immunity in experimental animals. *J. Exp. Med.* **174**, 1203–1208 (1991).
5. Kaslow, D. C. et al. A vaccine candidate from the sexual stage of human malaria that contains EGF-like domains. *Nature* **333**, 74–76 (1988).
6. Kaslow, D. C. et al. *Saccharomyces cerevisiae* recombinant Pfs25 adsorbed to alum elicits antibodies that block transmission of *Plasmodium falciparum*. *Infect. Immun.* **62**, 5576–5580 (1994).
7. Kumar, R., Angov, E. & Kumar, N. Potent malaria transmission-blocking antibody responses elicited by *Plasmodium falciparum* Pfs25 expressed in *Escherichia coli* after successful protein refolding. *Infect. Immun.* **82**, 1453–1459 (2014).
8. Gregory, J. A. et al. Algae-produced Pfs25 elicits antibodies that inhibit malaria transmission. *PLoS One* **7**, e37179 (2012).
9. Mlambo, G., Kumar, N. & Yoshida, S. Functional immunogenicity of baculovirus expressing Pfs25, a human malaria transmission-blocking vaccine candidate antigen. *Vaccine* **28**, 7025–7029 (2010).
10. Lee, S.-M. et al. Assessment of Pfs25 expressed from multiple soluble expression platforms for use as transmission-blocking vaccine candidates. *Malaria J.* **15**, 405 (2016).
11. Wu, Y. et al. Phase 1 trial of malaria transmission blocking vaccine candidates Pfs25 and Pvs25 formulated with Montanide ISA 51. *PLoS One* **3**, e2636 (2008).
12. Malkin, E. M. et al. Phase 1 vaccine trial of Pvs25H: a transmission blocking vaccine for *Plasmodium vivax* malaria. *Vaccine* **23**, 3131–3138 (2005).
13. Radtke, A. J. et al. Adjuvant and carrier protein-dependent T-cell priming promotes a robust antibody response against the *Plasmodium falciparum* Pfs25 vaccine candidate. *Sci. Rep.* **7**, 40312 (2017).
14. Shimp, R. L. Jr et al. Development of a Pfs25-EPA malaria transmission blocking vaccine as a chemically conjugated nanoparticle. *Vaccine* **31**, 2954–2962 (2013).
15. Miyata, T. et al. *Plasmodium vivax* ookinete surface protein Pvs25 linked to cholera toxin B subunit induces potent transmission-blocking immunity by intranasal as well as subcutaneous immunization. *Infect. Immun.* **78**, 3773–3782 (2010).
16. Gregory, J. A., Topol, A. B., Doerner, D. Z. & Mayfield, S. Alga-produced cholera toxin-Pfs25 fusion proteins as oral vaccines. *Appl. Environ. Microbiol.* **79**, 3917–3925 (2013).
17. Kumar, R. et al. Nanovaccines for malaria using *Plasmodium falciparum* antigen Pfs25 attached gold nanoparticles. *Vaccine* **33**, 5064–5071 (2015).
18. Kumar, R. et al. Potent functional immunogenicity of *Plasmodium falciparum* transmission-blocking antigen (Pfs25) delivered with nanoemulsion and porous polymeric nanoparticles. *Pharm. Res.* **32**, 3827–3836 (2015).
19. Jones, R. M. et al. A plant-produced Pfs25 VLP malaria vaccine candidate induces persistent transmission blocking antibodies against *Plasmodium falciparum* in immunized mice. *PLoS One* **8**, e79538 (2013).
20. Goodman, A. L. et al. A viral vectored prime-boost immunization regime targeting the malaria Pfs25 antigen induces transmission-blocking activity. *PLoS One* **6**, e29428 (2011).
21. Li, Y. et al. Enhancing immunogenicity and transmission-blocking activity of malaria vaccines by fusing Pfs25 to IMX313 multimerization technology. *Sci. Rep.* **6**, 18848 (2016).
22. Brune, K. D. et al. Plug-and-display: decoration of virus-like particles via isopeptide bonds for modular immunization. *Sci. Rep.* **6**, 19234 (2016).
23. Shao, S. et al. Functionalization of cobalt porphyrin–phospholipid bilayers with his-tagged ligands and antigens. *Nat. Chem.* **7**, 438–446 (2015).
24. Lee, S.-M., Plieskatt, J. & King, C. R. Disulfide bond mapping of Pfs25, a recombinant malaria transmission blocking vaccine candidate. *Anal. Biochem.* **542**, 20–23 (2018).
25. Rüger, R., Müller, D., Fahr, A. & Kontermann, R. E. In vitro characterization of binding and stability of single-chain Fv Ni-NTA-liposomes. *J. Drug Target.* **14**, 576–582 (2006).
26. Platt, V. et al. Influence of multivalent nitrilotriacetic acid lipid–ligand affinity on the circulation half-life in mice of a liposome-attached His6-protein. *Bioconj. Chem.* **21**, 892–902 (2010).
27. Bale, S. et al. Covalent linkage of HIV-1 trimers to synthetic liposomes elicits improved B cell and antibody responses. *J. Virol.* **91**, e00443-17 (2017).
28. Scally, S. W. et al. Molecular definition of multiple sites of antibody inhibition of malaria transmission-blocking vaccine antigen Pfs25. *Nat. Commun.* **8**, 1568 (2017).
29. Beck, Z. et al. Differential immune responses to HIV-1 envelope protein induced by liposomal adjuvant formulations containing monophosphoryl lipid A with or without QS21. *Vaccine* **33**, 5578–5587 (2015).
30. Sauer, S. W. & Keim, M. E. Hydroxocobalamin: improved public health readiness for cyanide disasters. *Ann. Emerg. Med.* **37**, 635–641 (2001).
31. Kuzminski, A. M., Del Giacco, E. J., Allen, R. H., Stabler, S. P. & Lindenbaum, J. Effective treatment of cobalamin deficiency with oral cobalamin. *Blood* **92**, 1191–1198 (1998).
32. Calabro, S. et al. Vaccine adjuvants Alum and MF59 induce rapid recruitment of neutrophils and monocytes that participate in antigen transport to draining lymph nodes. *Vaccine* **29**, 1812–1823 (2011).
33. Liang, F. et al. Vaccine priming is restricted to draining lymph nodes and controlled by adjuvant-mediated antigen uptake. *Sci. Transl. Med.* **9**, eaal2094 (2017).
34. Manh, T. P., Alexandre, Y., Baranek, T., Crozat, K. & Dalod, M. Plasmacytoid, conventional, and monocyte-derived dendritic cells undergo a profound and convergent genetic reprogramming during their maturation. *Eur. J. Immunol.* **43**, 1706–1715 (2013).
35. Ginhoux, F. et al. The origin and development of nonlymphoid tissue CD103$^+$ DCs. *J. Exp. Med.* **206**, 3115–3130 (2009).
36. Edelson, B. T. et al. Peripheral CD103$^+$ dendritic cells form a unified subset developmentally related to CD8α$^+$ conventional dendritic cells. *J. Exp. Med.* **207**, 823–836 (2010).
37. Rooijen, N. V. & Sanders, A. Liposome mediated depletion of macrophages: mechanism of action, preparation of liposomes and applications. *J. Immunol. Methods* **174**, 83–93 (1994).
38. Allen, T. M., Austin, G. A., Chonn, A., Lin, L. & Lee, K. C. Uptake of liposomes by cultured mouse bone marrow macrophages: influence of liposome composition and size. *Biochim. Biophys. Acta* **1061**, 56–64 (1991).
39. Fan, Y. C., Sahdev, P., Ochyl, L. J., Akerberg, J. J. & Moon, J. J. Cationic liposome–hyaluronic acid hybrid nanoparticles for intranasal vaccination with subunit antigens. *J. Control. Release* **208**, 121–129 (2015).
40. Cunningham, A. L. et al. Efficacy of the herpes zoster subunit vaccine in adults 70 years of age or older. *N. Engl. J. Med.* **375**, 1019–1032 (2016).
41. Viswanathan, S., Rani, C., Vijay Anand, A. & Ho, J. A. Disposable electrochemical immunosensor for carcinoembryonic antigen using ferrocene liposomes and MWCNT screen-printed electrode. *Biosens. Bioelectron.* **24**, 1984–1989 (2009).
42. Doolan, D. L. & Hoffman, S. L. DNA-based vaccines against malaria: status and promise of the Multi-Stage Malaria DNA Vaccine Operation. *Int. J. Parasitol.* **31**, 753–762 (2001).
43. Peterson, M. G. et al. Integral membrane protein located in the apical complex of *Plasmodium falciparum*. *Mol. Cell. Biol.* **9**, 3151–3154 (1989).
44. Lobo, C. A., Konings, R. N. & Kumar, N. Expression of early gametocyte-stage antigens Pfg27 and Pfs16 in synchronized gametocytes and non-gametocyte producing clones of *Plasmodium falciparum*. *Mol. Biochem. Parasitol.* **68**, 151–154 (1994).

Acknowledgements

This study was supported by PATH's Malaria Vaccine Initiative, and grants from the National Institutes of Health (R21AI122964 and DP5OD017898) and the intramural programme of the National Institute of Allergy and Infectious Diseases/NIH. The authors acknowledge assistance from G. Mlambo and A. Tripathi with immunofluorescence assays, and input from C. Alving and A. Birkett.

Author contributions

W.-C.H., C.R.K., S.-M.L. and J.F.L conceived the project. W.-C.H., K.M., S.-M.L. and J.F.L. designed most of the experiments. W.-C.H. and J.F.L. wrote the manuscript. W.-C.H., C.L. and J.G. performed the animal experiments. W.-C.H., C.L., B.D., C.A.L. and K.M. performed and interpreted the ELISA and SMFA experiments. A.R. and J.O. performed transmission electron cryomicroscopy. W.-C.H., K.A.C., C.L., X.H. and B.S. produced and characterized the liposomes. X.H. performed the splenocyte studies. U.C. and W.-C.H. produced fluorescently labelled antigens. J.F. performed the circular dichroism studies. S.D. and S.-M.L. produced the antigens.

Competing interests

W.-C.H., C.R.K., S.-M.L., J.G. and J.F.L are named inventors on a patent application describing this technology. All other authors declare no competing financial interests.

Additional information

Supplementary information is available for this paper at https://doi.org/10.1038/s41565-018-0271-3.

Reprints and permissions information is available at www.nature.com/reprints.

Correspondence and requests for materials should be addressed to J.F.L.

Publisher's note: Springer Nature remains neutral with regard to jurisdictional claims in published maps and institutional affiliations.

Methods

See the Supplementary Methods for additional details.

Materials. His-tagged Pfs25 was produced in a baculovirus system as previously described[10]. His-tagged plant-derived Pfs25 for enzyme-linked immunosorbent assay (ELISA) coating was produced in *Nicotiana benthamiana* as previously reported[45]. His-tagged Pfs230 was produced in a baculovirus system as previously reported[46]. His-tagged AMA-1 was produced in *Escherichia coli* as previously reported[47]. His-tagged Pfg27 (MRA-1274) was obtained from BEI Resources, and a $(NANP)_6$-$(His)_7$ peptide was synthesized by GenScript. CSP for ELISA was produced in *E. coli* as previously reported[48]. CoPoP was produced as previously described[23]. The following adjuvants were obtained: AddaVax (InvivoGen; catalogue number: vac-adx-10), Adju-Phos (InvivoGen; catalogue number: vac-phos-250), Quil-A (InvivoGen; catalogue number: vac-quil), TiterMax Gold Adjuvant (Sigma; catalogue number: T-2684), Sigma Adjuvant System (Sigma; catalogue number: S-6322), Imject IFA for the prime and CFA for the boost (Fisher; catalogue numbers: 77145 and 77140, respectively), Montanide ISA 720 (SEPPIC) and Alhydrogel 2% aluminium gel (Accurate Chemical And Scientific Corporation; catalogue number: A1090BS). The following lipids were used: DPPC (Corden; catalogue number: LP-R4-057), Ni-NTA lipid dioleoylglycero-Ni-NTA (Avanti; catalogue number: 790404P), 1,2-dioleoyl-*sn*-glycero-3-phosphocholine (Avanti; catalogue number: 850375), cholesterol (PhytoChol; Wilshire Technologies), PEG-lipid (DSPE-PEG2K; Corden; catalogue number: LP-R4-039), synthetic PHAD (Avanti; catalogue number: 699800P) and 3D6A (Avanti; catalogue number: 699855P). QS21 was obtained from Desert King. Granulocyte–macrophage colony-stimulating factor (GM-CSF) was obtained from Shenandoah Biotechnology (catalogue number: 200-15-AF). Cytochalasin B was obtained from Acros (catalogue number: 228090010).

Cell studies. RAW264.7 murine macrophage cells were obtained from the American Type Culture Collection and cultured in Dulbecco's modified Eagle's medium with 10% fetal bovine serum (FBS) and 1% penicillin/streptomycin.

BMDCs were derived from bone marrow cells obtained from CD-1 mice. Bone marrow was collected from the femurs and tibia of mice. The concentration of cells was seeded at 10^7 cells ml^{-1} and cultured in a 10 cm petri dish in Roswell Park Memorial Institute 1640 culture medium with 10% FBS and 20 ng recombinant GM-CSF on day 0. On day 3, an additional 10 ml medium containing GM-CSF was added to the petri dish to give a final volume of medium of 20 ml. On day 6, non-adherent cells were collected and cultured in a 24-well plate at 5×10^5 cells ml^{-1} in Roswell Park Memorial Institute culture medium containing 10% FBS and 1% penicillin/streptomycin, then incubated for 24 h with CoPoP/PHAD, CoPoP and phosphate buffered saline (PBS) mixed at 1 μg ml^{-1} Pfs25, with a fixed CoPoP:Pfs25 mass ratio of 4:1. Cells were washed with PBS containing 0.1% bovine serum albumin (BSA) three times and stained with antibodies against CD11c, CD40, CD80 and MHC-II for 1 h on ice before flow cytometry.

For the in vitro uptake studies, RAW264.7 cells and BMDCs (5×10^5 well^{-1}) were cultured in a 24-well plate overnight to reach 70–80% confluence. Cells were then either: (1) treated with various types of liposomes with 1 μg ml^{-1} of Pfs25-488; or (2) pre-incubated with cytochalasin B (10 μg ml^{-1}) for 1 h before the uptake study. For quantification, after incubation for 4 h, the cells were harvested, washed with PBS three times and treated with lysis buffer (1% Triton X-100 and 0.1% sodium dodecyl sulfate in PBS). The fluorescence signal was measured and the cellular Pfs25 uptake was calculated by first preparing a Pfs25-488 standard curve and calculating the concentration based on the standard curve.

Liposome preparation. Liposomes were prepared by ethanol injection and nitrogen-pressurized lipid extrusion in PBS. This procedure was carried out at 60 °C followed by dialysis to remove the ethanol. For liposomes containing QS21, the QS21 (1 mg ml^{-1}) was added to the liposomes after formation at a mass ratio equal to PHAD. The final liposome concentration was adjusted to 320 μg ml^{-1} PHAD and the solution was passed through a 0.2 μm sterile filter and stored at 4 °C. Liposome sizes and polydispersity indices were determined by dynamic light scattering with a NanoBrook 90Plus PALS instrument after 200-fold dilution in PBS. The standard CoPoP/PHAD liposome formulation had a mass ratio of DPPC:cholesterol:PHAD:CoPoP of 4:2:1:1. Other formulations are detailed in the Supplementary Information.

SNAP characterization. Protein binding with Pfs25 or lysozyme (VWR; catalogue number: 97062-138) was carried out by incubating protein and liposomes with a 1:4 mass ratio of protein:PHAD, unless otherwise stated. Following incubation, the sample was subjected to microcentrifugal filtration (Pall; catalogue number: 29300), and protein in filtrate was assessed by Micro BCA (Thermo Fisher Scientific; catalogue number: 23235). For gel electrophoresis, loading dye was added to liposome samples, loaded into PAGE gels (Lonza; catalogue number: 8522) and subjected to electrophoresis and staining. Cryogenic transmission electron microscopy was carried out as described in the Supplementary Information. Samples for immunization were prepared in the same way, but diluted in PBS to achieve the desired antigen dosing, with the antigen:PHAD mass ratio remaining constant (1:4).

SNAP multiplexing. Multiplexing was carried out by mixing CoPoP/PHAD liposomes with five different his-tagged malaria antigens (Pfs25, Pfs230, Pfg27, AMA-1 and NANP) for 3 h at room temperature in the same way as Pfs25. A constant mass ratio of antigen:PHAD of 1:4 was maintained in all cases.

Murine immunization and serum analysis. CD-1 mice (8 wk old, female) received intramuscular injections on days 0 and 21 containing the indicated antigen doses combined with the indicated adjuvants. Serum was collected on day 42 unless otherwise indicated and sent to the Laboratory of Malaria and Vector Research at the National Institute of Allergy and Infectious Diseases for anti-Pfs25 ELISA[49] and SMFA[50,51] analysis, which were carried out as previously described. Supplementary Tables 1–5 report the raw SMFA data.

Rabbit immunization. New Zealand white rabbits (10–12 wk old, female) received intramuscular injections on days 0 and 28 of 1 or 10 μg Pfs25 adjuvanted with CoPoP/PHAD (4 or 40 μg PHAD) liposomes or 10 μg Pfs25 with alum. Serum samples were collected on days 0, 28 and 56. Serum was sent to the National Institute of Allergy and Infectious Diseases for ELISA and SMFA analysis.

Flow cytometry. Flow cytometry studies were carried out using a BD LSRFortessa X-20 flow cytometer. FlowJo (version 10) software was used for data analysis.

For the draining lymph node studies of Pfs25 uptake in immune cells, mice were intramuscularly immunized with 1 μg of Pfs25-488 conjugate. Then, 2 d after injection, they were killed and inguinal lymph nodes were collected. Cells were extracted and fixed with 4% paraformaldehyde at room temperature for 15 min, then washed three times with 3 ml PBS under centrifugation at 500 r.c.f. for 5 min. Some 5×10^5 cells per tube were stained for 30 min at room temperature with murine antibodies against I-A/I-E, B220, CD11c or F4/80 (all from BioLegend).

To stain marrow cells, on day 250, mice were killed and bone marrow was collected. Marrow cells were counted, fixed with 4% paraformaldehyde at room temperature for 15 min in the dark, washed three times with PBS and frozen in 10% dimethyl sulfoxide. Cells were stained with anti-CD138 and anti-B220 antibodies (BioLegend) for 30 min at room temperature in the dark, followed by three PBS washes. Cells were permeabilized with 0.1% Triton X-100 and stained with Pfs25-488, followed by additional washing before flow cytometry.

For the germinal centre cells and Tfh cell populations, mice received 100 ng Pfs25 adjuvanted with CoPoP/PHAD or alum. Then, 14 d after immunization, the mice were killed and the inguinal lymph nodes were collected. Cells extracted from the lymph nodes were fixed with 4% paraformaldehyde for 15 min at room temperature, and washed three times with 3 ml PBS under centrifugation at 500 r.c.f. for 5 min. Some 5×10^5 cells per tube were than stained for 1 h on ice with antibodies against B220, CD95, GL7, CD4, CXCR5 or PD-1 before flow cytometry.

For lymph node cell recruitment, mice were injected intramuscularly with CoPoP/PHAD liposomes or alum with 100 ng of Pfs25. Then, 48 h after injection, the mice were killed and lymph nodes were collected for cell extraction. Cells were fixed with 4% paraformaldehyde for 15 min at room temperature and washed with PBS three times. Cells were stained with a combination of antibodies against Ly6C, CD11b, Ly6G, CD11c, CD3, I-A/I-E and F4/80 for 1 h on ice. Cells were first gated with CD11c and CD11b (Supplementary Fig. 8a). Then, immune cells were identified based on surface markers in $CD11c^{high}$ and $CD11b^{low}$, neutrophils ($Ly6G^{high}$; Supplementary Fig. 8d), eosinophils ($Ly6G^{int}$, $F4/80^{int}$ and side scatter; Supplementary Fig. 8e), monocytes ($Ly6C^{high}$; Supplementary Fig. 8c) and macrophages ($F4/80^{high}$; Supplementary Fig. 8b). Three types of dendritic cells were gated (Supplementary Fig. 8f). For myeloid dendritic cells, we first gated $Cd11c^{high}$- and $CD11b^{high}$-positive cells, and then MHC-II-positive cells.

Acute toxicity studies. CD-1 mice (8 weeks old, female) were treated with an intramuscular injection of CoPoP/PHAD/Pfs25 prepared in the usual way with 20 μg Pfs25, or with intravenous injection of CoPoP/PEG liposomes (95:5 molar ratio of CoPoP:PEG) at 100 mg kg^{-1} CoPoP. Two weeks later, blood and serum were collected and subjected to standard complete blood cell count and serum panels (IDEXX; catalogue number: 98-20590-00). Organs, including the kidney, lung, liver and spleen, were fixed in formalin for 24 h, then transferred to 70% ethanol and subjected to haematoxylin and eosin staining. Briefly, slides were de-waxed through xylenes and graded alcohols; transferred to water for 3 min, haematoxylin for 3 min, water for 3 min, 1% acid alcohol for 1 min, water for 3 min, 0.2% ammonium hydroxide for 3 min, water for 4 min, 95% ethanol for 3 min and eosin for 30 s; and then dehydrated through graded alcohols, cleared, mounted and coverslipped with xylene mount before imaging.

Indirect immunofluorescence assay. *P. falciparum* schizonts, gametocytes, ookinetes and sporozoites were obtained and fixed on slides as described in the Supplementary Methods. Slides were blocked with 5% BSA in PBS containing 0.1% Tween-20 for 30 min at 37 °C. Serum collected from mice immunized with individual or multiplexed antigens with SNAP or alum was diluted 1:100 and incubated in 5% BSA in PBS with the fixed slides at 37 °C for 1 h, followed by three washes with PBS in a humidity chamber, each time for 5 min. Fluorescein isothiocyanate-conjugated goat anti-mouse IgG (1:1000) was then incubated with the slides for 30 min at 37 °C, followed by three washes with PBS, each time for 5 min.

The slides were mounted with ProLong Gold Antifade with 4′,6-diamidino-2-phenylindole (DAPI; Thermo Fisher Scientific; catalogue number: P36931) and imaged with an EVOS FL microscope using a 100× objective lens.

Ethics. All experiments involving mice were carried out using protocols approved by the University at Buffalo Institutional Animal Care and Use Committee. All experiments involving rabbits were carried out using protocols approved by the Pocono Rabbit Farm Institutional Animal Care and Use Committee.

Data availability

All raw data are available upon request.

References

45. Farrance, C. E. et al. Antibodies to plant-produced *Plasmodium falciparum* sexual stage protein Pfs25 exhibit transmission blocking activity. *Hum. Vaccin.* **7**, 191–198 (2011).
46. Lee, S. M. et al. An N-terminal Pfs230 domain produced in baculovirus as a biological active transmission-blocking vaccine candidate. *Clin. Vaccine Immunol.* **24**, e00140-17 (2017).
47. Dutta, S. et al. High antibody titer against apical membrane antigen-1 is required to protect against malaria in the Aotus model. *PLoS One* **4**, e8138 (2009).
48. Genito, C. J. et al. Liposomes containing monophosphoryl lipid A and QS-21 serve as an effective adjuvant for soluble circumsporozoite protein malaria vaccine FMP013. *Vaccine* **35**, 3865–3874 (2017).
49. Miura, K. et al. Development and characterization of a standardized ELISA including a reference serum on each plate to detect antibodies induced by experimental malaria vaccines. *Vaccine* **26**, 193–200 (2008).
50. Quakyi, I. A. et al. The 230-kDa gamete surface protein of *Plasmodium falciparum* is also a target for transmission-blocking antibodies. *J. Immunol.* **139**, 4213–4217 (1987).
51. Cheru, L. et al. The IC_{50} of anti-Pfs25 antibody in membrane-feeding assay varies among species. *Vaccine* **28**, 4423–4429 (2010).